Journal of South American Earth Sciences 140 (2024) 104922

Contents lists available at ScienceDirect

Journal of South American Earth Sciences

journal homepage: www.elsevier.com/locate/jsames

Anomalous behaviour of fine-grained transition soils from the San Cayetano Formation (Loja, Ecuador)

Carmen Esparza [a], Francisco Lamas [b,*], John Soto [a], Jose Miguel Azañón [c,d], Patricia Ruano [c,d], José Tamay [a], Francisco José Martínez-Moreno [e], Jesús Galindo-Zaldívar [c,d]

[a] *Universidad Técnica Particular de Loja, San Cayetano Alto, PO Box 11-01-608, Loja, Ecuador*
[b] *Civil Engineering Department, E.T.S Ingeniería de Caminos, Canales y Puertos, University of Granada, 18071, Granada, Spain*
[c] *Department of Geodynamics, Faculty of Sciences, University of Granada, 18071, Granada, Spain*
[d] *Instituto Andaluz de Ciencias de la Tierra (CSIC-University of Granada), Faculty of Sciences, 18071, Granada, Spain*
[e] *Departamento de Geodinámica, Estratigrafía y Paleontología, Facultad de Ciencias Geológicas, Universidad Complutense de Madrid, 28040, Madrid, Spain*

A R T I C L E I N F O

Keywords:
Geotechnical characterization
Stress-strain behavior
Quasi-nonlinear model
Finite element methods
Ecuadorian Andes

A B S T R A C T

Numerous landslides, either natural or produced by excavations in road works, occur in the intramontane Neogene Loja basin (southern Ecuadorian Andes) and can be associated with the clayey silts, low plasticity soils (ML). Thirty-two undisturbed samples from eight sites were tested in laboratory to characterize the stress-strain geotechnical soil response, showing a higher internal friction angle and higher cohesion with respect to the standard ML soil values. A testing profile of a road constructed on these soils has been modeled using finite element methods to calculate both the safety factor and the mechanism of evolution. Anomalous behavior is evidenced when a standard ML soil type is considered in the model, with a higher security factor than the less stable and more susceptible ML soils of Loja basin. Therefore, this contribution may serve as a warning to designers and engineers when constructing new structures on these soils. Additionally, it enables the identification of the most effective test for assessing high susceptibility in ML soils, contributing to the refinement and enhancement of methodological procedures during project execution.

1. Introduction

The classification of a soil is necessary for comparisons with other soils of the same group, hence providing a fast reference about its geotechnical behavior (Mitchell and Soga, 2005; Young, 2012). The Corps of American Engineers enhanced a soil classification system (Casagrande, 1947) based on the Airfield Classification System. Subsequently, the Bureau of Reclamation adopted and designated this system as the Unified Soil Classification System (USCS) (Turnbull et al., 1952). All civil engineers worldwide currently use this geotechnical classification method. The soils are classified into different groups, each having different engineering properties. The classification criteria are:

a) Percentage of gravel, sand, and fine soils according to the grain size.
b) Texture and maximum size of the granulometric curve for coarse-grained soils.
c) Plasticity and compressibility of fine-grained soils and organic soils.

In grouping similar soils with regard to their engineering general behavior, the USCS classification uses "group symbols".

Slope stability models (Dapena, 1993; Lamas et al., 2014; Wong and Duncan, 1974) are based on the definition of geotechnical parameters typical of each material. These parameters may be obtained by performing laboratory tests of samples from representative undisturbed soil samples (ASTM, 2007), which evidence the real behavior, although the process is costly and time-consuming. Alternatively, they can be taken directly from values given in tables for different types of soils, which implies some uncertainty about the accuracy of the results. Therefore, the Soil Classification (Casagrande, 1947; ASTM, 2007) provides, a priori, useful information on soils from quick and cheap tests at the initial studies, reducing costs and time and constitute the base to order more accurate tests.

Numerous landslides affect the intramontane Neogene Loja Basin (Ecuador). This basin is located in the southern Ecuadorian Andes, formed as result of subduction of the Nazca plate below the continental

* Corresponding author
E-mail addresses: caesparza@utpl.edu.ec (C. Esparza), flamas@ugr.es (F. Lamas), jesoto@utpl.edu.ec (J. Soto), jazanon@ugr.es (J.M. Azañón), pruano@ugr.es (P. Ruano), jvtamay@utpl.edu.ec (J. Tamay), fjmmoreno@ucm.es (F.J. Martínez-Moreno), jgalindo@ugr.es (J. Galindo-Zaldívar).

https://doi.org/10.1016/j.jsames.2024.104922
Received 20 October 2023; Received in revised form 17 April 2024; Accepted 26 April 2024
Available online 27 April 2024

crust of the South American Plate (Alvarado et al., 2016; Tamay et al., 2018; Ramos, 2021) (Fig. 1). A very rugged relief owing to tectonic deformation characterizes this area, with related recent and active structures associated to seismicity (Tamay et al., 2018). Loja basin is filled with Middle and Upper Miocene sedimentary detritic rocks, discordantly overlying, a basement made up of metapelitic rocks of Chiguinda and Tres Lagunas Fm., with local igneous intrusions (Aspden et al., 1992; Laffaldano and Bunge, 2008; Hungerbühler et al., 2002). The sedimentary infill began with fluvial, deltaic and lacustrine deposits grouped in the northwestern part of the basin (from bottom to top) into the Trigal, La Banda, and Belen formations, which correspond in eastward to the San Cayetano Formation. All these rocks are covered by the Quillollaco formation (Galindo-Zaldívar et al., 2010).

Loja Basin is located in the upper catchment area of the Zamora River. It is characterized by a Humid Subtropical climate with no dry season (according to climate classification of Köppen, 1936) and Ecuadorian meteorological service (Soto et al., 2017), influenced by the interaction of the Amazonia and the trade winds related to Pacific Ocean marine currents and the Peruvian desert. Its temperature fluctuates between 14 °C and 24 °C. Precipitation occurs throughout the year, being especially predominant in the months of December to April. The annual average rainfall amounts to 895.2 mm.

The San Cayetano formation is composed of conglomerates, sandstones and lutites. Most of the instabilities recognized in the Loja region occur in the soils of the San Cayetano formation (Fig. 2). However, they are used as cores of numerous embankments of the Ecuadorian road network.

The aim of this research is to study the mechanical behavior of fine-

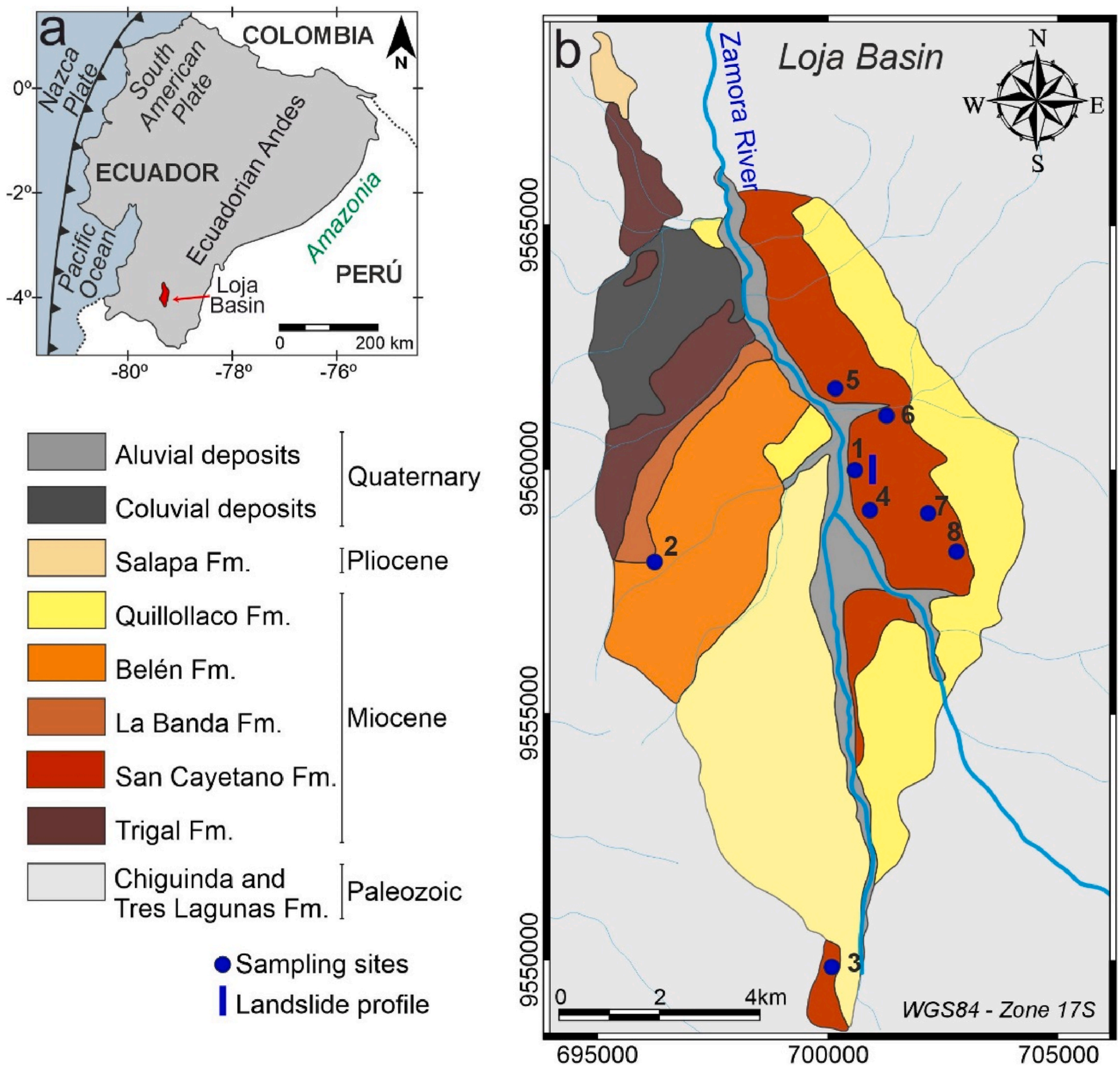

Fig. 1. Geographic and geological setting of Loja Basin (a), and location of the analyzed sampling sites on the lithological map of the basin (b). Modified from Tamay et al. (2016).

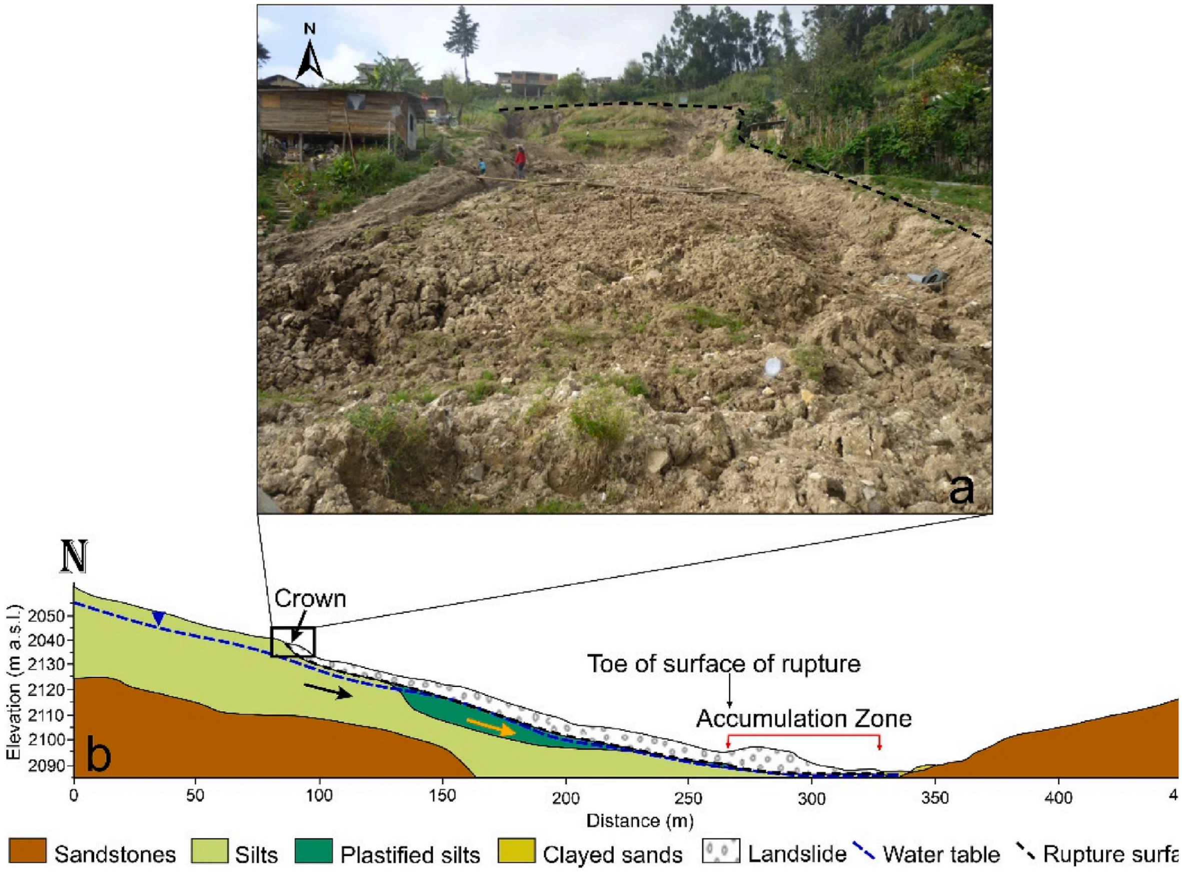

Fig. 2. Studied landslide of Loja Basin. (a) Field view of the landslide crown. (b) Geological profile. The digital elevation model was generated using public municipal available data. The DTM has a resolution of 10 m per pixel.

grained transitional soils, very common in the South American continent, used in embankments and excavations, in comparison with the behavior of standard soils that would correspond to those of the USCS classification. For this purpose, the geotechnical properties of these soils that were extracted in the San Cayetano Formation were determined and the stress-strain behavior was evaluated based on the hyperbolic model (Lamas et al., 2011). The analysis was conducted on a real profile of a landslide from the San Cayetano Formation. In the first step, the analysis considered the actual geotechnical parameters of these study soils. In the second step, the analysis takes into account the standard parameters of clayey silts low plasticity soils (ML). Clear differences were observed in their evolution and in the calculated safety factors. This suggests an anomalous behavior of the San Cayetano soils compared to the features expected from a standard ML soil. We will also discuss the implications of this behavior for use in South American road network slope stability models, particularly regarding the definition of typical geotechnical parameters for these soils.

2. Methodology

2.1. Field and laboratory procedures

Soil sampling was carried out in the Loja Basin (Ecuador). A first selection of the most suitable sites for sampling was carried out after a detailed field survey of the area. We have avoided shallow sampling sites that may be altered due to anthropic activities, vegetation or very shallow processes. The best sites for sampling are located in recent anthropic road and building trenches at depths relative to the surface comprised between 3 and 10 m (Fig. 1). The samples were extracted with soil samplers according to the standard protocol AENOR XP-P-94-202, ASTM D 1587, and prepared following ASTM D 421 (ASTM, 2007). Samples were covered with bandages and liquid paraffin to preserve their natural characteristics until their analysis and testing at the laboratories of the University of Granada (Spain); ASTM D 421 (ASTM, 2007). We tested 32 undisturbed specimens from eight areas considered very representative of the soils under study.

To avoid loss of density and moisture, the samples were always handled in a humid chamber. Some specimens required prior preparation, performed by compacting to natural moisture using a mini Harvard compactor in 5 layers and compacted with a Harvard hammer with 12 blows per layer, in a mould with a diameter of 1.5 inches and a height of 3.0 inches (Lamas et al., 2002; Wilson, 1950). The organic matter content has been calculated according to the standard UNE 103204:10.

For geotechnical characterization, the standards outlined in Eurocode 7 (2016) were employed. These include specifications for index properties such as particle size distribution and consistency, as detailed by the granulometric curve (UNE 103-101-95), Atterberg limits (UNE 103-103-94), and plasticity index (UNE 103-104-93). Performance of oedometric trials (UNE 74527) allowed further estimations of the swelling of the samples, following the free-swell submersion technique according to "Technical Committee on expansive soils" (ISSMFE, 1987). The triaxial tests carried out were type CU with preliminary consolidation, break without drainage, and measurement of pore pressures (UNE 103402).

The choice of this type of test is justified by the low permeability of the soils studied as well as the importance of determining the pore pressure. The consolidation tests were carried out on submerged samples, and the duration of the load steps was normalized to 24 h to ensure full primary consolidation.

In addition, to obtain residual parameters for the area of study, a ring shear test was used, drained and consolidated on samples remoulded according to ASTM D 6467-06 (AASHTO, 2002). This type of assay allows very large deformations to be reached without loss of cross-section.

The chemical composition of the samples was determined with fractions passing through the No. 10 sieve (ASTM) using inductively coupled plasma mass spectrometer (ICP-MS) for analysis of the major elements on total dry sample. Electronic X-ray fluorescence and diffraction was also used to determine the mineralogical composition. The texture was studied with a Philips PW1710 diffractometer. Warshaw and Roy (1961) proposed the procedure used for determining the clay mineral. The results of the chemical analysis were studied together with mineralogical data to arrive at the global composition.

To obtain the stress-strain relationship of the materials, after triaxial and oedometer tests, we used the hyperbolic model described by Wong and Duncan (1974), following the methodology described by Lamas et al. (2011) (Supplementary material).

Permeability was calculated using a standard technique (Rowe and Barden, 1966) with a triaxial cell and a head-base pressure gradient (U. S. Bureau of Reclamation, 1980). The quantity of organic matter was determined by analysis with potassium permanganate in an acid medium, applying a quantitative standard method.

2.2. Finite element methods (FEM) techniques

When possible, soil classification should be performed according to methods that are simple to achieve in a short time, inexpensive, and entailing a small number of variables.

We calculated and compared the mechanism of breakage and the sliding safety factor on a slope accurately measured in the study area (Fig. 2), with the geotechnical parameters of the samples studied and those of the type ML soil, to check if the classification system proposed is valid for the analysis of the studied soils. The stability study uses FEM techniques (Supplementary material).

3. Results

To verify the correctness of the soil classification for San Cayetano, it was considered using as a reference another soil with a very similar texture, which had been tested in previous investigations (Lamas et al., 2014). This soil was defined as a brown sandy clay loam of medium plasticity, with 22% fine sand, subangular fine ash, primarily composed of quartz, and corresponding to the ML group. The geotechnical parameters of this soil are presented in Supplementary Table 1.

The studied landslide occurs in a peri-urban area. A road cuts across the landslide for a distance of 100 m. The selected profile for finite element method (FEM) modeling is situated along the maximum slope of the entire landslide, representing the most unfavourable condition. This profile extends for a length of 280 m and reaches a maximum height difference of 75 m, affecting an area of 2.5 ha.

The Supplementary Table 2 presents the results of the field analysis of samples that have been developed according to Jamiolkowsky et al. (1985). We have decided not to include the samples from sampling sites 4 and 5 (Fig. 1 and Supplementary Table 2) in the study due to their high content of organic matter (>50%), which produced a completely different behavior from the others and did not contribute anything to the purpose of the study.

3.1. Geochemical and mineralogical composition of the material

The results of the chemical analysis of specimen's representative of the study areas, given in Supplementary Table 3, leads us to highlight:

- Al_2O_3 and K_2O indicates the presence of kaolinite and illite clays (Bergaya and Lagaly, 2006).
- Fe_2O_3 can come from both clay minerals and oxides and to a lesser degree from sulphides. Likewise, MgO characterizes clay minerals as well as dolomite. With respect to the clay minerals, Fe_2O_3 and MgO are associated with the smectites, transformed by the sedimentation processes (Troalen, 1994). Therefore, we can relate these results with the possible expansivity of the samples.
- The CaO comes from the carbonates and gypsum. As shown in Supplementary Table 3, there is a total correlation between the content of CaO with the carbonate concentration, as expected. The gypsum concentration in our samples is not representative.
- The SiO_2 characterizes mainly the mineral quartz and other silicates including silicate clays. High contents of SiO_2 are observed with a marked uniformity among areas.

X-ray diffraction showed the samples to be mainly composed of quartz and clays with traces of dolomitic material, with all the alumina forming part of three-layer clay in the fine material. Supplementary Table 4 also reflects the similarity among areas.

3.2. Index properties

The soil of the areas tested passes through the 2 mm sieve and the fine soils lie in a wider range, from 96.98% for sampling site 1, to 22.76% for sampling site 7 (Fig. 3). All the samples contain only sand and fine aggregate, the sandy content found in ranges from 3.02% in sampling site 1–77.24% in sampling site 7, being entirely fine sand.

The fine fraction comprises silts and clays which, according to the results of diffractometry, are mainly montmorillonite and illite, showing a greater presence in sampling site 1 where the clay content is above 40%, while in sample 7 the clay content is about 5.4%. The rest of the fine fraction is mostly quartz.

There is a clear reciprocity between Atterberg's limits (liquid limit and plasticity index) with the mineralogical composition, presenting cohesion in all the studied soils. Although the distribution reveals two differentiated areas, the samples were not significantly different (Supplementary Table 5).

According to the plasticity and sand content (Supplementary Table 5), the samples are located in the classes of CL, ML, CL-ML and due to its high content in sand the sample EC-7 (70%) is classified as SM. They can be described as a silt, or sandy silt of low plasticity.

The variability in compaction obtained among areas was larger than for the other index parameters (Supplementary Table 6). The density varies between 0.12 and 0.03, with moisture between 3.45 and 0.64. This variability can be explained by the different sand content in the samples. The density of the samples exhibits a maximum value of 2.02 T/m^3 (sampling site 7), and a minimum of 1.72 T/m^3 (sampling site 2).

Taking into account the results of the index properties, these soils are categorized according to the Unified Soil Classification System (USCS).

Of the fine fraction from the areas studied in the charter of plasticity (Fig. 4), almost all belong to the class of low plasticity. The exceptions are sampling site 6, which either has a clearly silty behavior or one of silt and clay having very low plasticity, and sampling site 7, situated clearly in a sandy area given the amount of the sand fraction. The classification of Loja Basin soils according to USCS is included in Supplementary Table 7.

Under this classification, the soils of the San Cayetano formation mostly belong to "ML" category. According to the Bureau of Reclamation's study on 'The Field Identification Procedures', this soil type falls under the category of 'Silt, non-plastic; contains a slight amount of very fine sand'. More precisely, it can be classified as plastic sandy clayey silt, characterized by 19.82% of subangular sand content, exhibiting a wet and consolidated state in its natural location. There are differences between the classification obtained in the field and the one obtained with laboratory data. This is due to differences between the techniques used in the field and those indicated by laboratory regulations. Although initially it would seem that, the first is more legitimate (the field procedure being less standardized); the discrepancy serves as a starting point for schedule the subsequent laboratory study.

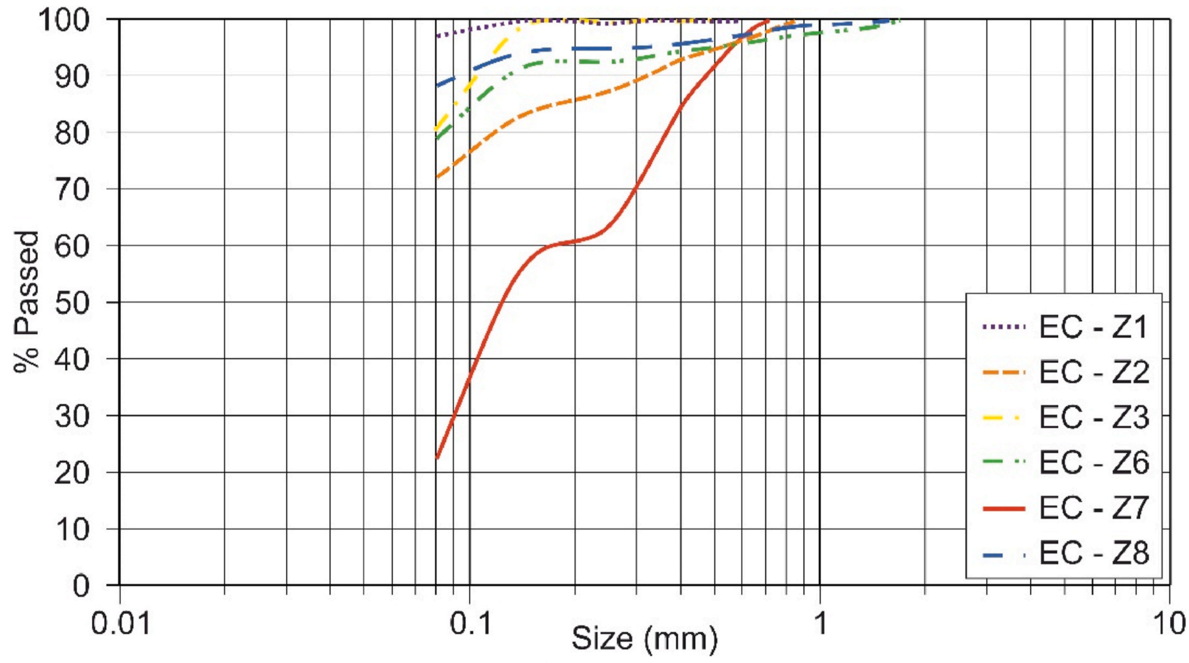

Fig. 3. Granulometric curves of the sampling sites.

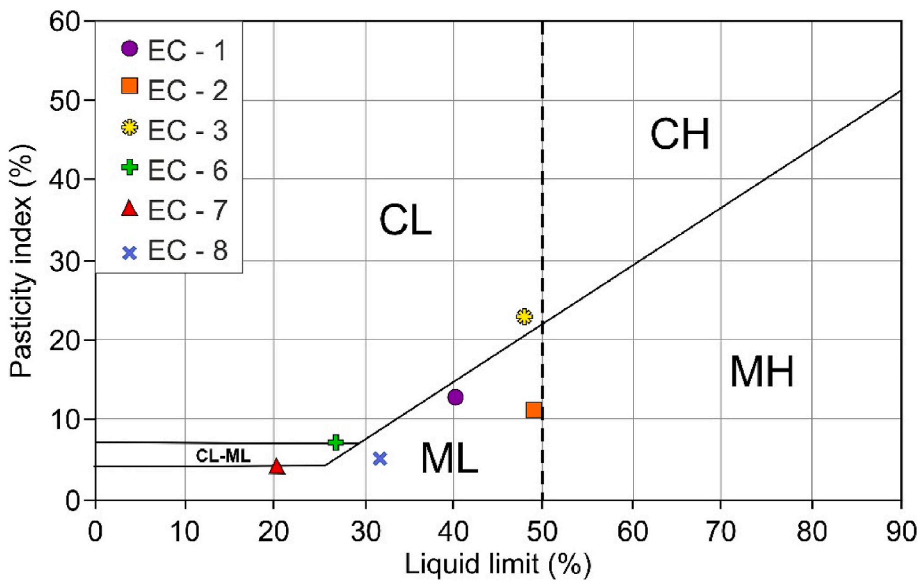

Fig. 4. Plasticity chart including the main fields of the Unified Soil Classification System (USCS). In sample EC-7, due to its high sand content (70%), only the fine fraction is plotted.

3.3. Mechanical properties

The failure parameters present values for the effective internal friction angle, which ranges between 22.2° and 36°, defining ductile to ductile-fragile behavior according to the sand content (Supplementary Table 8).

The Consolidated undrained triaxial (CU) test (Fig. 5) is used to determine peak parameters, while the annular test (Fig. 6) is better suited for obtaining residual parameters. The annular test allows for achieving significant deformations without compromising the cross-sectional integrity, ensuring that the true residual state of the soil is reached.

The angles of effective internal friction residuals have very low values (Supplementary Table 9).

For sampling sites 4 and 5 no data are presented because of the peat contents of organic matter greater than 50%. This soil poses no risk to destabilizing construction, as its colour makes it easy to identify and remove during embankment execution.

Oedometric test results are presented in Fig. 7, which provide the results of consolidation and permeability parameters shown in Supplementary Table 10. The C_V values were compared with those obtained using the empirical relationships with Atterberg limits. The values thus obtained were found to be significantly lower in all relations used, although the relationships using the initial pore index and natural moisture give values too high.

In Supplementary Table 10, permeability was included because its dependence on the consolidation can be clearly evidenced. Half of the studied soils have high compressibility, typical of fine-grained soils,

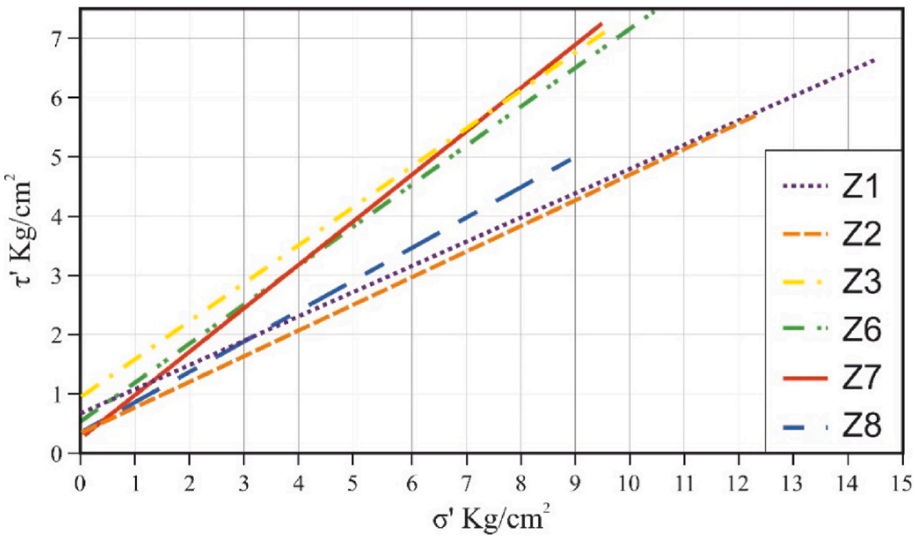

Fig. 5. Consolidated undrained triaxial (CU) test results.

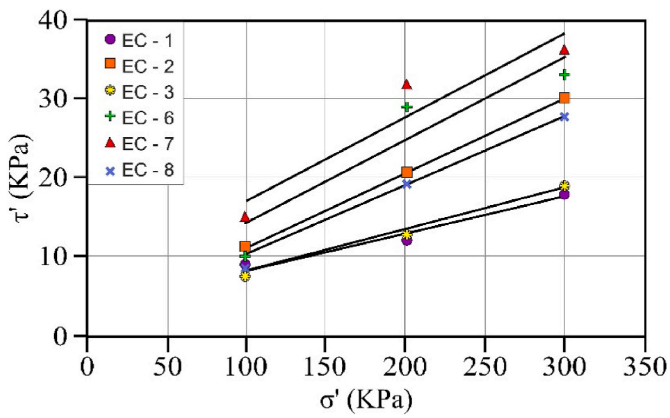

Fig. 6. Ring shear test results.

including cohesive ones, and mixtures of sand, clay and silt of medium compatibility; the permeability coefficient values are in the range of 2.01 E^{-05} cm/s to 1.17 E^{-06} cm/s, although most specimens are closer to the lower extreme.

Stress-strain parameters (E', G', K', R_f, n, k_{ur} and {') were calculated (Supplementary Table 11) from the model equations, considering the formulas already defined in the methodology (Dapena, 1993; Lamas et al., 2011), following the hypotheses formulated by St. John et al. (1992) and the deviatory stress-strain curves.

According to hyperbolic model (Supplementary material), the results of triaxial testing were used for the parameters k, n and R_f. The rate of R_f values with respect to the density are comprised between 0.57 and 0.99, however, most have a quite uniform value of 0.99.

The initial modulus of elasticity is plotted against the dry density (Fig. 8). This is explained by the difference of textures and degrees of consolidation, with values from 81.66 to 980.4 MPa. However, no clear relationship between density and the modulus of initial elasticity is observed in this context.

The values of Poisson's ratio show no significant variations among areas. This is logical given the small variation that Poisson's ratio generally presents for similar soils. Thus, the value of G = 0.64 was taken as the average. These values are typical of clayey sands that are cohesive, dense, highly consolidated, with fragile elastic characteristics, susceptible to breakage with little deformation —coherent values according to Wong and Duncan (1974) and Lamas et al. (2011).

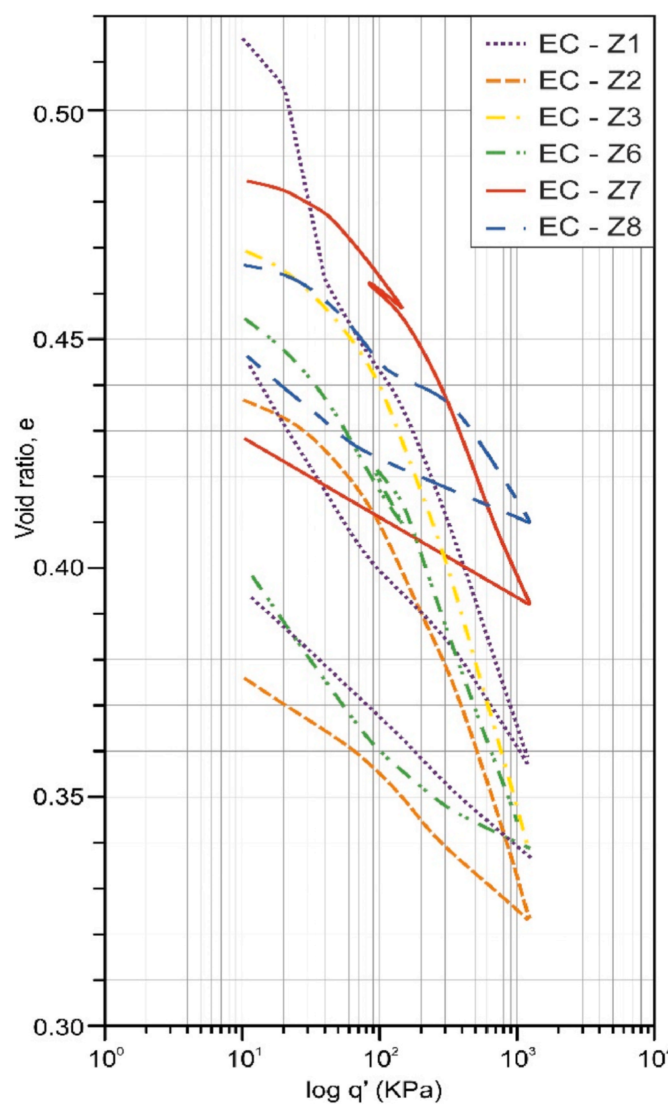

Fig. 7. One – dimensional compression oedometric test results.

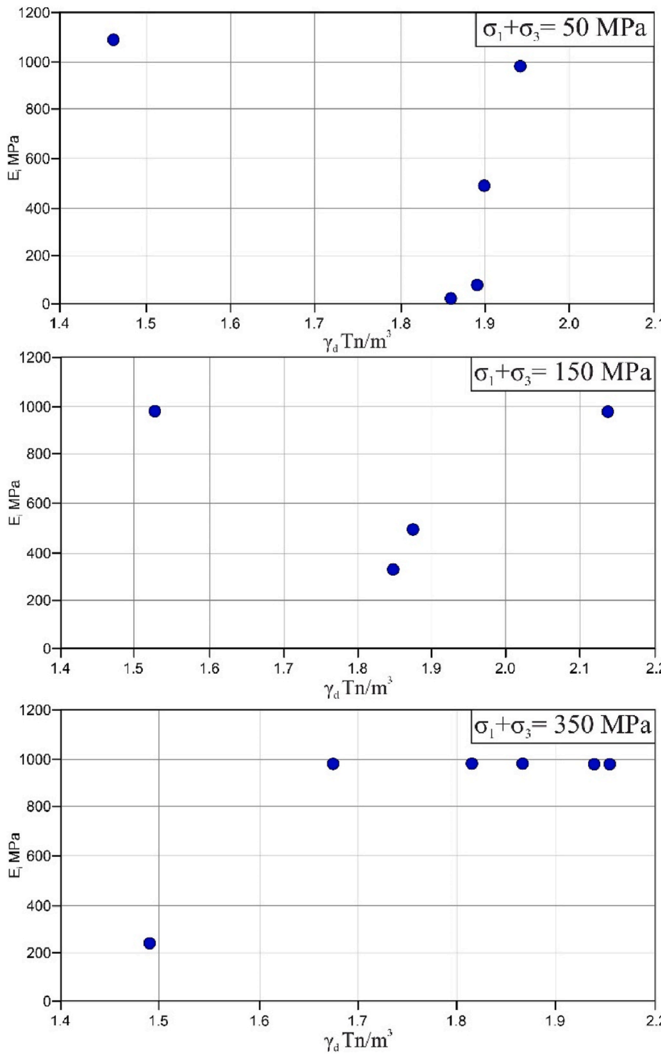

Fig. 8. Relationship, Ei module versus γd, for different confining pressures.

3.4. Stress-strain behavior model by FEM

Calculations of the models were performed using PLAXIS (2010) software. Two models have been developed considering standard ML soils and San Cayetano formation soils average values (Table 1) taking the following model characteristics: Plane Strain; mesh element: triangular 15 nodes to give an acceptable period of computation and good precision, with 395 active elements and 3367 nodes of computation giving a size to each node of 9.574 m on average. The computation sheet, steps: 275 of 275; step type: Consolidation; Kernel type: 32 bits; Extrapolation factor: 2000; Relative stiffness: 1000. Consolidation: Realised P Excess, Max: 0.07048×10^{-75} kN/m^2. The digital elevation model was generated using public municipal available data. The DTM has a resolution of 10 m per pixel.

Table 1
Soils type to the study.

Parameter	Standard soil	San Cayetano Soils (average)	Units
©*d*	17.0	18.1	kN/m^3
©*sat*	20.0	19.1	kN/m^3
e	0.43	0.4	
L.L.	45.0	40.5	%
P.L.	34.5	12.64	%
%<0.08 mm	70.3	73.41	%
Sand	25.7	23.59	%
Size Max.	4.0	3.0	mm
USCS	ML	ML	

A partial refining in the deformation zone was carried out for the more critical silt of San Cayetano areas. All calculations were made considering the most unfavourable conditions, represented by a degree of consolidation of 90%, which is understood to be the beginning of secondary consolidation or fluency. The input data for materials are the parameters calculated in the previous sections for samples (Supplementary Table 2) and the material data type ML (Supplementary Table 1).

Four phases of calculation are defined in each case. In the first phase of 90% consolidation, the increased effective stress as well as pore pressure reduction are studied. In the second phase, the variation of the consolidation is studied. In the third phase, the dissipation of the pore pressure is calculated at the end of the cycle. Finally, in the fourth phase, the safety factor of the final profile is calculated using the parameter *ΣMsf*.

In both cases, using standard and native soil models, we modeled a circular failure surface based on the initial data and in-situ profile analysis (Fig. 2). Furthermore, considering the calculated parameters, the observed behavior exhibits a ductile-brittle response. The water table is situated at a depth greater than 10 m, and the triggering factor for the failure event was attributed to the heavy rainfall that occurred in the preceding month, with 150 mm of precipitation over a 15-day period, as reported by state authorities, in conjunction with ongoing road construction work. Comparison of the deformed final profile with San Cayetano soils (Fig. 9a) and with ML standard soils (Fig. 9b) reveals different behavior and safety factors. Silts of San Cayetano reach a safety factor value of 1.08, which under the methodology described means unstable; whereas with type ML data, the obtained value of 2.56 would be clearly stable.

4. Discussion

In the Loja Basin, the primary issue with San Cayetano soils lies in the stability of the road network. The analysis of various sample characteristics is aimed at enhancing efficiency and identifying the best procedures for analyzing these soils, thereby improving the quality of their geomechanical characterization. If successful, this approach would contribute to design more coherent test campaigns, ultimately saving time and costs.

The angle of friction is higher than expected in samples from sampling site 8 (Figs. 1 and 5 and Supplementary Table 8), which is somewhat anomalous considering that the behavior is preferentially ductile. Regarding cohesion, the data presented are consistent, though somewhat higher for sand content. This may be due to the presence of smectites-type minerals, common in all areas. The residual effective internal friction angles are lower than the standard values according to the lithology. The presence of clay minerals — that fall totally in the plastification zone — impede an increase of these angles (Fig. 6 and Supplementary Table 9).

These results are consistent with those of Moore (1991) and Skempton (1985), confirming the correlation of the residual strength with the type of clay and the content of fine sand; still, dependence appears to be quite complex and involve other variables, such as interstitial water and pore size. According to Hawkins and McDonald (1992), the fraction of silt size would govern the dependency between pore water and residual effective angle.

The greater preconsolidation pressure than the maximum pressure reached in the past can be attributed to the unions formed during secondary consolidation and other physics-chemical factors (Dapena, 1993). An accurate determination of the preconsolidation pressure is an important step in predicting long-term stability, settlement analysis and consolidation procedures (Jamiolkowski et al., 1985; Lamas et al., 2014).

The calculation of the hyperbolic model parameters relied on triaxial

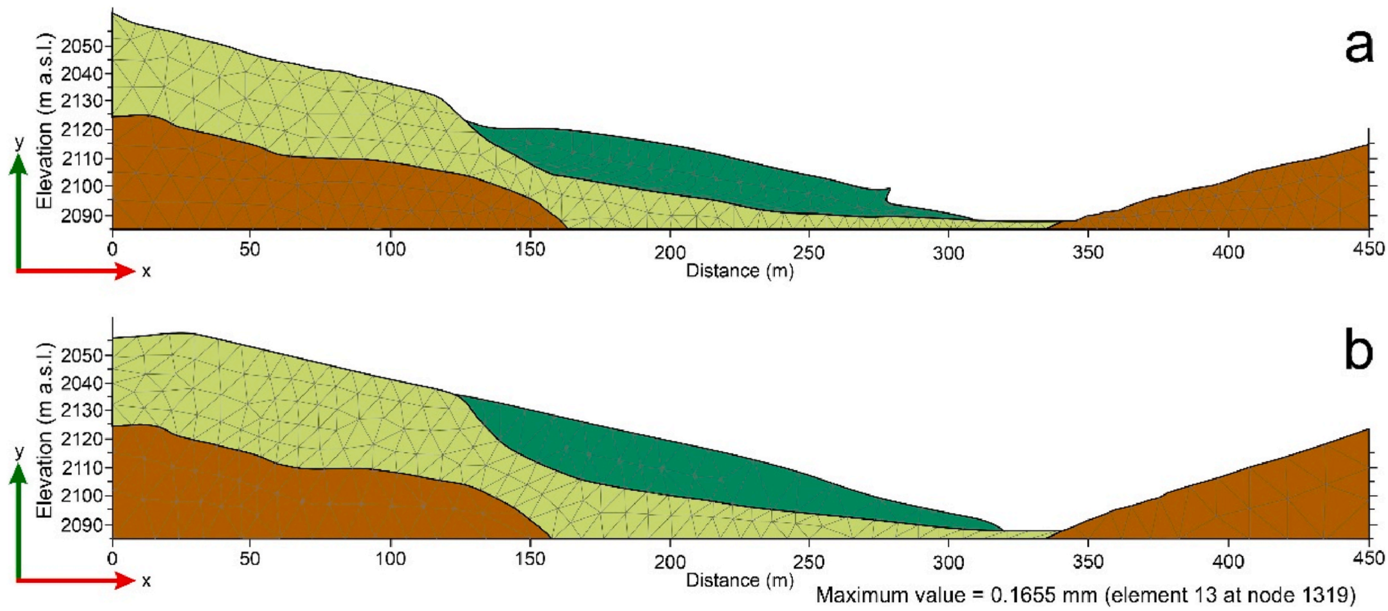

Fig. 9. Final deformed mesh (a) San Cayetano soils and (b) Standard ML (USCS) soils (Table 1).

tests of the CU type, with previous consolidation, undrained breakage and pore pressure measurements, since determining impermeability and pore pressure variations requires the use of this type of test.

Although the results are quite consistent with the expected behavior, there are poor correlations between the dry density versus the modulus of rupture and also in respect to the initial elasticity module. One possible reason is the relationship between the mechanical behavior and the texture-composition of the soil.

The texture, mineralogy, cementation, consolidation, index properties, and mechanical parameters of these soils determine their mechanical behavior during compression and deformation. This behavior evidences the contrast characteristics when compared Loja Basin soils and standard ML soils. The types of breaks in the studied San Cayetano soil are much more brittle and their mechanical behavior is closer to dense sands than to standard ML cohesive soils. The slope stability mechanisms for the Loja Basin landslide profile, calculated with FEM, give different results for these soils than for the standard ML types, and the factor of safety is also much lower for these soils. Their mineralogical composition produces a rather complex mechanical relationship.

5. Conclusions

To enhance our understanding of ML soil behavior, with a specific focus on the anomalous characteristics exhibited by the San Cayetano Formation, we conducted an analysis of the classification and geotechnical properties of the soils of this formation. This silty formation is located in the intramontane Neogene Loja basin, situated in southern Ecuador. Tests were performed on 32 undisturbed samples from eight areas.

Mineral content of these soils is mainly quartz (from 39% to 17%); illite (14%–54%); montmorillonite (4.9%–7.8%); kaolinite (3%–22%); and muscovite (12%–21%) (Supplementary Table 4). The soils are of low to medium plasticity, although their behavior is more like a dense sand than a cohesive soil, given the high content in quartz and that the overall average density was 1.80 T/m^3. These soils have marked impermeability, preconsolidation pressure, and vertical consolidation coefficients, corroborating the above; oedometric studies indicate no swelling.

San Cayetano soils display a distinct mechanical behavior in comparison to standard soils, which can be attributed to the presence of materials like quartz and other minerals typically considered that doesn't cause or promote any change in the soil's geotechnical properties. These materials, in combination with plasticity and granulometry values characteristic of ML soils, lead to significantly higher effective internal friction angles. This, in turn, results in an unexpected decrease in the safety factor of landslides developed in San Cayetano soils, posing significant challenges for slope stability studies in the region.

CRediT authorship contribution statement

Carmen Esparza: Writing – original draft, Methodology, Investigation, Formal analysis, Conceptualization. **Francisco Lamas:** Writing – original draft, Methodology, Investigation, Data curation, Conceptualization. **John Soto:** Resources, Investigation, Funding acquisition, Formal analysis, Data curation, Conceptualization. **Jose Miguel Azañón:** Validation, Supervision, Formal analysis, Conceptualization. **Patricia Ruano:** Visualization, Supervision, Conceptualization. **José Tamay:** Validation, Resources, Conceptualization. **Francisco José Martínez-Moreno:** Writing – review & editing, Data curation. **Jesús Galindo-Zaldívar:** Writing – original draft, Resources, Methodology, Funding acquisition, Formal analysis, Data curation, Conceptualization.

Declaration of competing interest

The authors declare that they have no known competing financial interests or personal relationships that could have appeared to influence the work reported in this paper.

Data availability

Data will be made available on request.

Acknowledgements

We are grateful for the comments of two anonymous reviewers who have helped to improve the quality of this contribution and the editor Prof. Samaniego. This work was supported by the research groups, RMN 241, RNM 148, and project PID2022-136678NB-I00 financed by MICIU/AEI 10.13039/501100011033 and FEDER, UE, and the Universidad Técnica Particular de Loja, Ecuador, are acknowledged for the funding and facilities behind this work.

Appendix A. Supplementary data

Supplementary data to this article can be found online at https://doi.org/10.1016/j.jsames.2024.104922.

References

AASHTO, 2002. Standard Specifications for transportation materials and methods of sampling and testing: Part I. Specifications. In: American Association of State Highway and Transportations Officials, fourteenth ed. 444 North Capitol St. N. W. Suite 225, Washington, DC.

Alvarado, A., Audin, L., Nocquet, J.M., Jaillard, E., Mothes, P., Jarrín, P., et al., 2016. Partitioning of oblique convergence in the Northern Andes subduction zone: migration history and the present-day boundary of the North Andean Sliver in Ecuador. Tectonics 35, 1048–1065.

Aspden, J.A., Fortey, N., Litherland, M., Viteri, F., Harrison, S.M., 1992. Regional S-type granites in the Ecuadorian Andes: possible remnants of the breakup of western Gondwana. J. S. Am. Earth Sci. 6, 123–132.

ASTM, 2007. Standard Test Method for Particle-Size Analysis of Soils. ASTM international, West Conshohocken, PA.

Bergaya, F., Lagaly, G., 2006. General introduction: clays, clay minerals, and clay science. Developments in clay science 1, 1–18.

Casagrande, A., 1947. Classification and identification of soils. Proceedings ASCE 73 (6), 1947, 783-810.

Dapena, E., 1993. Comportamiento Tenso – Deformacional de un Suelo Arcilloso para Núcleo de Presa. Simposio Nacional sobre Geotecnia de Presas de Materiales Sueltos. 1 (4), 84-604-7839-4. 87 – 96. Zaragoza (España).

Eurocode 7, 2016. Geotechnical Design - Part 2: the Laboratory Test. CTN 140/SC 7 – GEOTECNIA. European Standardization Committee.

Galindo-Zaldívar, J., Soto, J., Ruano, P., Tamay, J., Lamas, F., Guartán, J., Azañón, J.M., Paladines, A., 2010. Geometría y estructuras de la cuenca neógena de Loja a partir de datos gravimétricos (Andes Ecuatorianos). Geogaceta 48, 215–218.

Hawkins, A., McDonald, C., 1992. Decalcification and residual shear strength reduction in fuller's earth clay. Geotechnique 42, 3453–3464.

Hungerbühler, D., Steinmann, M., Winkler, W., Sewards, D., Egüez, A., Peterson, D.E., Helg, U., Hammer, C., 2002. Neogene stratigraphy and Andean geodynamics of southern Ecuador. Earth Sci. Rev. 57, 75–124.

ISSMFE, 1987. Evaluation of swelling pressure of expansive soil in laboratory. Draft Standard. Technical committee on expansive soils. International Society for Soils Mechanics and foundation Engineering TC6, 1–5.

Jamiolkowsky, M., Ladd, C.C., Germaine, J.T., Lancellotta, R., 1985. New developments in field and laboratory testing. 11th Znt. Conf. SMFE 1, 57–153.

Köppen, W., 1936. Das geographische System de Klimate. Handbuch der klimatologie. Gebrüder Borntraeger, Berlin, Germany, pp. pp1–44.

Laffaldano, G., Bunge, H.P., 2008. Strong plate coupling along the Nazca–South America convergent margin. Geology 36, 443–446.

Lamas, F., Irigaray, C., Chacón, J., 2002. Geotechnical characterization of carbonates marls for the construction of impermeable dam cores. Eng. Geol. 66, 283–294.

Lamas, F., Lamas-López, F., Bravo, R., 2014. Influence of carbonate content of marls used in dams: geotechnical and statistical characterization. Eng. Geol. 177, 32–39.

Lamas, F., Oteo, C., Chacón, J., 2011. Influence of carbonate content on the stress – strength behavior of Neogene marls from the Betic cordillera (Spain) in cu triaxial tests using quasilinear elastic (hyperbolic) model. Eng. Geol. 122, 160–168.

Mitchell, J.K., Soga, K., 2005. Fundamentals of Soil Behavior, vol. 3. John Wiley & Sons, USA, New York.

Moore, R., 1991. The chemical and mineralogical controls upon the residual strength of pure and natural clay. Geotechnique 41, 35–47.

PLAXIS, 2010. Computation program version 2D. In: Wilde. Delft University, Netherlands.

Ramos, V.A., 2021. Fifty years of plate tectonics in the Central Andes. J. S. Am. Earth Sci. 105, 102997.

Rowe, P.W., Barden, L.A., 1966. New consolidation cells. Geotechnique 16, 162–170.

Skempton, A.W., 1985. Residual strength in landslides, holed strata and laboratory. Geotechnique 35, 1–18.

Soto, J., Galve, J.P., Palenzuela, J.A., Azañón, J.M., Tamay, J., Irigaray, C.A., 2017. Multi-method approach for the characterization of landslides in an intramontane basin in the Andes (Loja, Ecuador). Landslides 14, 1929–1947.

St John, H.D., Potts, D.M., Jardine, R.J., Higgins, K.G., 1992. Prediction and performance of ground response due to construction of a deep basement at 60 Victoria embankment. Proceedings of Wroth Memorial Symposium. Oxford, pp. 581–608.

Tamay, J., Galindo-Zaldívar, J., Ruano, P., Soto, J., Lamas, F., Azañón, J.M., 2016. New insight on the recent tectonic evolution and uplift of the southern Ecuadorian Andes from gravity and structural analysis of the Neogene-Quaternary intramontane basins. J. S. Am. Earth Sci. 70, 340–352.

Tamay, J., Galindo-Zaldívar, J., Martos, Y.M., Soto, J., 2018. Gravity and magnetic anomalies of ecuadorian margin: implications in the deep structure of the subduction of Nazca Plate and Andes Cordillera. J. S. Am. Earth Sci. 85, 68–80.

Troalen, J.P., 1994. Constant ultrastructural et comportment des géomatériaux. Bull. Int. Assoc. Eng. Geol. 49, 73–83.

Turnbull, W.J., Boyd, W.K., Foster, C.R., Griffith, J.M., Ray, O.B., ARMY ENGINEER WATERWAYS EXPERIMENT STATION VICKSBURG MS, 1952. Design of Flexible Airfield Pavements for Multiple-Wheel Landing Gear Assemblies. Report Number 1. Test Section with Lean Clay Subgrade.

U.S. Bureau of Reclamation, 1980. Earth Manual. U.S. Department of Interior. U.S. Government Printing Office, Washington, DC.

Warshaw, C.H., Roy, R., 1961. Classification and scheme for the identification of layer silicates. Bull. Geol. Soc. Am. 72, 1455–1492.

Wilson, S.D., 1950. Small soil compaction apparatus duplicates field results closely. Eng. News Rec. 145, 34–36.

Wong, K., Duncan, J.M., 1974. Hyperbolic Stress – Strain Parameters for Nonlinear Finite Elements Analysis of Stresses and Movements in Soils Masses. University of California, Berkeley, California. Report nº TE – 44 – 3.

Young, R.N., 2012. Soil Properties and Behavior, vol. 5. Elsevier.